Many-body Bose systems and the hard-sphere model: dynamic properties from the weak to the strong interaction regime

2014 J. Phys.: Conf. Ser. 529 012022

(http://iopscience.iop.org/1742-6596/529/1/012022)

Journal of Physics: Conference Series **529** (2014) 012022 doi:10.1088/1742-6596/529/1/012022

Many–body Bose systems and the hard-sphere model: dynamic properties from the weak to the strong interaction regime

R Rota [1], F Tramonto[2], D E Galli[2] and S Giorgini[1]

[1] Dipartimento di Fisica and INO-CNR BEC Center, Università degli Studi di Trento, via sommarive 14, 38123 Trento, Italy

[2] Dipartimento di Fisica, Università degli Studi di Milano, via Celoria 16, 20134 Milano, Italy

E-mail: rota@science.unitn.it

Abstract. We obtain *ab-initio* estimations of the dynamic structure factor, $S(\mathbf{q},\omega)$, of Bose gases at zero temperature. More precisely, we use the Genetic Inversion via Falsification of Theories (GIFT) algorithm to perform analytic continuations of imaginary time correlation functions computed via an exact Path Integral projector method. Using the hard-sphere potential to model the two-body interactions between the atoms, we compute $S(\mathbf{q},\omega)$ changing the gas parameter from the dilute regime ($na^3 = 10^{-4}$) up to the density corresponding to superfluid ^{4}He at equilibrium ($na^3 = 0.2138$). With increasing density, we observe the emergence of a broad multiphonon contribution accompanying the quasiparticle peak and a crossover of the dispersion of elementary excitations from a Bogoliubov-like spectrum to a phonon-maxon-roton curve. Apart from the low wave vector region, for $na^3 = 0.2138$ the energy-momentum dispersion relation and the static density response function, $\chi(\mathbf{q})$, turns out to be in good agreement with the superfluid ^{4}He experimental data at equilibrium density.

1. Introduction

The study of the collective modes and the dynamic properties of ultracold gases has always represented a very important issue in quantum many-body theories. In particular, in the case of Bose systems, this study is fundamental to understand the phenomenon of superfluidity and, starting from the pioneering studies of Landau and Bogoliubov in the 1940s, it has been subject of a huge number of works, both theoretical and experimental [1].

A physical insight on the dynamic behavior of quantum many-body systems can be given estimating the dynamic structure factor, $S(\mathbf{q},\omega)$. This quantity, indeed, contains a wealth of information about the nature and the energy spectrum of the excitations coupled to density fluctuations and, for a system made up of N particles described by the Hamiltonian $\hat{H}$, at zero temperature it can be written as:

$$S(\mathbf{q},\omega) = \frac{1}{2\pi N}\int_{-\infty}^{+\infty} dt\; e^{i\omega t}\frac{\langle\Psi_0|\rho_{-\mathbf{q}}(t)\rho_{\mathbf{q}}(0)|\Psi_0\rangle}{\langle\Psi_0|\Psi_0\rangle} = \frac{1}{N}\sum_{n\geq 0}\delta\left(\omega - \frac{E_n - E_0}{\hbar}\right)\frac{|\langle\Psi_n|\rho_{\mathbf{q}}|\Psi_0\rangle|^2}{\langle\Psi_0|\Psi_0\rangle}, \quad (1)$$

where $\rho_{\mathbf{q}}(t) = e^{i\hat{H}t/\hbar}\rho_{\mathbf{q}}e^{-i\hat{H}t/\hbar}$ is the time evolution of the density fluctuation operator $\rho_{\mathbf{q}} = \sum_{i=1}^{N} e^{-i\mathbf{q}\cdot\mathbf{r}_i}$ and $|\Psi_0\rangle$ is the ground state of the many-body system. Equivalently, introducing

a complete set of eigenstates $|\Psi_n\rangle$, $S(\mathbf{q},\omega)$ can be expressed in terms of all the excited states which have non–zero overlap with the density perturbation, $\rho_{\mathbf{q}}|\Psi_0\rangle$, as in the right term of Eq. 1.

For dilute gases at low temperature, we can safely assume that the s-wave scattering length, a, is much smaller than the mean inter-particle distance, $n^{-1/3}$ (being n the density of the gas), and the ground state of the many-body system can be described in terms of a macroscopic wave function [2]. In this regime, mean-field theories are expected to provide an accurate description of the system and the elementary excitations can be expressed in terms of a single quasiparticle. Therefore, the dynamic structure factor reduces to a single peak, whose dispersion follows the Bogoliubov spectrum

$$\varepsilon_B(\mathbf{q}) = \frac{\hbar^2}{2m\xi^2}\sqrt{(q\xi)^4 + 2(q\xi)^2}\ , \tag{2}$$

in which $\xi = 1/\sqrt{8\pi n a}$ is the healing length. This result, predicted for the first time in 1947, has been confirmed experimentally in 2002 by Steinhauer *et al.*, who have been able to measure the excitation spectrum of a dilute condensate of ^{87}Rb atoms by means of Bragg spectroscopy [3].

As the density of the system increases, the interactions among the particles become more and more important and the picture provided by mean-field theories is no longer valid. Indeed, experimental measurements [4, 5, 6, 7, 8, 9] of the dynamic structure factor in liquid ^{4}He, that is a well-known benchmark of a dense Bose fluid, show a different behavior from the one predicted for dilute systems. First of all, the $S(\mathbf{q},\omega)$ in liquid ^{4}He presents, in addition to a sharp "quasiparticle" peak, a broad contribution at higher frequencies, usually called multiphonon branch, that indicates the possibility to induce incoherent excitations in the many-body system. Furthermore, the dispersion of the main peak of $S(\mathbf{q},\omega)$ differs from the Bogoliubov spectrum, Eq. 2, and presents a phonon-maxon-roton behavior, which is linear at low q and displays a relative minimum for a non-zero wave vector.

To perform a reliable study of strongly interacting Bose gases, it is fundamental to develop many-body theories able to include all the relevant correlations among the particles. For instance, *ab-initio* numerical techniques based on Quantum Monte Carlo (QMC) simulations have been widely used to calculate "exactly" the equilibrium properties of dense Bose fluids, such as superfluid ^{4}He, both at zero [10] and finite temperature [11]. Nevertheless, the study of the dynamic properties of quantum many-body systems by means of QMC methods has to face the problem of analytical continuation from purely imaginary to real time of the correlation function entering the Fourier transform in Eq. 1, which strongly limits any possibility of a precise determination of $S(\mathbf{q},\omega)$. Several methods have been developed in order to extract information about the real-time dynamics of quantum systems from the limited and noisy data achievable in QMC simulations. The most popular one is the Maximum Entropy (ME) method, a stochastic technique based on the bayesian inference [12]. ME has been used in the study of several physical systems, but it provides only qualitative results when applied in the analysis of quantum fluids [13, 14]. Recently, a powerful algorithm called Genetic Inversion via Falsification of Theories (GIFT) has been proposed; this algorithm can provide very accurate results for liquid and solid ^{4}He, being able to recover both the sharp quasiparticle peak and the multiphonon branch, each with the correct relative spectral weight [15].

In this work, we want to study, by means of QMC methods, the dynamic properties of Bose gases at zero temperature, focusing on the crossover from weak to strong interaction regime. To model the interactions among the particles, we use the two-body hard-sphere (HS) potential

$$V(r) = \begin{cases} \infty & (r \le a) \\ 0 & (r > a) \end{cases}\ , \tag{3}$$

where the range of the potential a coincides with the s-wave scattering length. This model has been widely used for the study of many-body systems with short-range repulsive interactions,

not only in the dilute regime, where the details of the interatomic potential are irrelevant, but also in the dense regime [16, 17, 18, 19]. The HS model, indeed, serves as a reference for those systems in which the leading part of the two-body potential is the repulsive hard-core at short distances and it has been used to characterize semi-quantitatively the static properties of superfluid ^{4}He [17, 18]. Moreover, the HS model provides one with a well defined system, where quantum correlations can be investigated from the weak to the strong interaction regime by varying a single parameter, i.e. the reduced density in units of the HS range.

The structure of the paper is as follows. In Section 2 we introduce the numerical methods used in our study, namely the Path Integral Ground State (PIGS) method, applied to the calculation of the imaginary-time correlation functions, and the GIFT algorithm, for the estimation of the dynamic structure factors from the PIGS data. In Section 3 we show our results for the dynamic structure factor, for the dispersion law of the elementary excitations and for the static density response function. Finally, in Section 4 we draw our conclusions.

2. Numerical Methods

2.1. Path Integral Ground State method

In this work, we use the Path Integral Ground State (PIGS) method [10] to evaluate ground-state expectation values of static and imaginary time dynamic properties of the many-body system. PIGS is a QMC algorithm in which the many-body ground state wave function $\Psi_0(\mathrm{R})$ is expressed as an evolution in imaginary time of a trial wave function $\Psi_T(\mathrm{R})$, where $\mathrm{R} = \{\mathbf{r}_i\}_{i=1}^N$ represents the set of the positions of the N particles. Indeed, if the trial state is not orthogonal to the ground state, the imaginary time evolution operator $e^{-\tau\hat{H}}$ acts on Ψ_T, allowing the exponential decay of any overlap with the excited states with respect to the overlap with Ψ_0. Thus, when the imaginary time τ is large enough, it projects $\Psi_T(\mathrm{R})$ onto the ground-state wave function, according to the formula

$$\frac{\Psi_0(\mathrm{R})}{\sqrt{\langle\Psi_0 \mid \Psi_0\rangle}} = \lim_{\tau\to\infty} \mathcal{N}_\tau \int d\mathrm{R}'\, G(\mathrm{R},\mathrm{R}';\tau)\,\Psi_T(\mathrm{R}')\ , \tag{4}$$

where $\mathcal{N}_\tau$ is a τ–dependent normalization factor and $G(\mathrm{R},\mathrm{R}';\tau) = \langle \mathrm{R}|e^{-\tau\hat{H}}|\mathrm{R}'\rangle$ is the imaginary time propagator.

In general, $G(\mathrm{R},\mathrm{R}';\tau)$ is not known, but it is possible to develop analytical expressions which approximate it accurately in the limit of short imaginary times [11, 20, 21, 22]. For this reason, it is convenient to rewrite the propagator in Eq. 4 as a convolution of M propagators $G(\mathrm{R}_l,\mathrm{R}_{l+1};\delta\tau)$ on a short time $\delta\tau = \tau/M$. Making use of a certain scheme to approximate $G(\mathrm{R}_l,\mathrm{R}_{l+1};\delta\tau)$, we are able to obtain an accurate analytical form for the ground state wave function

$$\frac{\Psi_0(\mathrm{R_M})}{\sqrt{\langle\Psi_0 \mid \Psi_0\rangle}} \simeq \mathcal{N}_\tau \int d\mathrm{R}_1 \ldots d\mathrm{R}_{M-1} \prod_{l=0}^{M-1} G(\mathrm{R}_l,\mathrm{R}_{l+1};\delta\tau)\,\Psi_T(\mathrm{R}_0)\ , \tag{5}$$

and finally we are able to calcualte a generic expectation value $\langle\Psi_0\,|\hat{O}|\Psi_0\rangle$ as a statistical average over many random sets of $2M+1$ configurations, $\{\mathrm{R}_l\}_{l=0}^{2M}$, obtained by sampling the probability density

$$p(\mathrm{R}_0,\mathrm{R}_1,\ldots,\mathrm{R}_{2M}) = \mathcal{N}_\tau^2\,\Psi_T(\mathrm{R}_0) \prod_{l=0}^{2M-1} G(\mathrm{R}_l,\mathrm{R}_{l+1};\delta\tau)\Psi_T(\mathrm{R}_{2M})\ , \tag{6}$$

with a Metropolis-like algorithm. In order to sample correctly and efficiently the Bose symmetry of the ground-state wave function, we adopt a canonical worm algorithm [20, 23]. For Bose systems, the PIGS method can be considered "exact": indeed, controlling the parameters M and $\delta\tau$, it is possible to systematically improve the accuracy of Eq. 5 and to reach a regime in

which the approximations affect the numerical results to an extent which is below the statistical error.

Even though PIGS results do not depend on the approximation for the imaginary time propagator and on the trial wave function used [20, 24], a wise choice of these two ingredients can notably increase the efficiency of the algorithm. In our work, we use the pair-action approximation for the propagator at short imaginary times [11, 25, 26]:

$$G(\mathrm{R},\mathrm{R}',\delta\tau) \simeq G_0(\mathrm{R},\mathrm{R}',\delta\tau)\prod_{i<j}\frac{g_{rel}(\mathbf{r}_{ij},\mathbf{r}'_{ij},\delta\tau)}{g^0_{rel}(\mathbf{r}_{ij},\mathbf{r}'_{ij},\delta\tau)} \ . \tag{7}$$

Here, $G_0(\mathrm{R},\mathrm{R}',\delta\tau)$ is the N-particle free propagator, $g_{rel}(\mathbf{r}_{ij},\mathbf{r}'_{ij},\delta\tau)$ is the two-body propagator of the interacting system, which depends on the relative coordinates $\mathbf{r}_{ij}=\mathbf{r}_i-\mathbf{r}_j$ and $\mathbf{r}'_{ij}=\mathbf{r}'_i-\mathbf{r}'_j$, and $g^0_{rel}(\mathbf{r}_{ij},\mathbf{r}'_{ij},\delta\tau)$ is the free propagator for two particles. In the study of the HS system, it is convenient to approximate the two-body interacting propagator with its high energy expansion, proposed for the first time by Cao and Berne [22]:

$$\frac{g_{rel}(\mathbf{r},\mathbf{r}',\delta\tau)}{g^0_{rel}(\mathbf{r},\mathbf{r}',\delta\tau)} = 1-\frac{a(r+r')-a^2}{rr'}e^{-m[rr'+a^2-a(r+r')](1+\cos\theta)/(2\hbar^2\delta\tau)} \ , \tag{8}$$

where θ is the angle between $\mathbf{r}$ and $\mathbf{r}'$, $r=|\mathbf{r}|$ and $r'=|\mathbf{r}'|$.

As trial wave function, we choose the translationally invariant Jastrow wave function

$$\Psi_T(\mathrm{R}) = \prod_{i<j} f(|\mathbf{r}_i-\mathbf{r}_j|) \ , \quad \text{with } f(r)=\begin{cases} 0 & (r\le a) \\ \frac{\sin[k(r-a)]}{r} & (r>a) \end{cases} \ . \tag{9}$$

The function f is the solution of the two-body s-wave scattering problem with a HS potential and the wave vector k is chosen such as the derivative $f'(r)$ vanishes at $r=L/2$, where L is the size of the cubic simulation box, in order to fulfill the periodic boundary conditions [19].

2.2. GIFT algorithm

With the PIGS method described above, we can obtain the imaginary time intermediate scattering function, $F(\mathbf{q},\tau)$, i.e. the imaginary time correlation function of the density fluctuation operator, $\hat{\rho}_{\mathbf{q}}=\sum_{i=1}^{N}e^{-i\mathbf{q}\cdot\hat{\mathbf{r}}_i}$:

$$F(\mathbf{q},\tau) = \frac{1}{N}\frac{\langle\Psi_0|e^{\tau\hat{H}}\hat{\rho}_{-\mathbf{q}}e^{-\tau\hat{H}}\hat{\rho}_{\mathbf{q}}|\Psi_0\rangle}{\langle\Psi_0\mid\Psi_0\rangle} \ . \tag{10}$$

This quantity is related to the dynamic structure factor, $S(\mathbf{q},\omega)$, via the Laplace transform

$$F(\mathbf{q},\tau) = \int_0^\infty d\omega\ e^{-\omega\tau}\,S(\mathbf{q},\omega) \ . \tag{11}$$

Therefore, if we want to estimate $S(\mathbf{q},\omega)$ from the PIGS data for $F(\mathbf{q},\tau)$, it is necessary to invert this integral equation.

However, the inversion of Eq. 11 is a well-known ill-posed problem: indeed, given the smoothing nature of the kernel $\mathcal{K}(\omega,\tau)=e^{-\omega\tau}$, several spectral functions $S(\mathbf{q},\omega)$, even with very different features, can give similar results for $F(\mathbf{q},\tau)$. Furthermore, we have to notice that, in QMC simulations, $F(\mathbf{q},\tau)$ is accessible only in correspondence of a finite number of imaginary time values affected by statistical uncertainties. As a consequence, there exists an

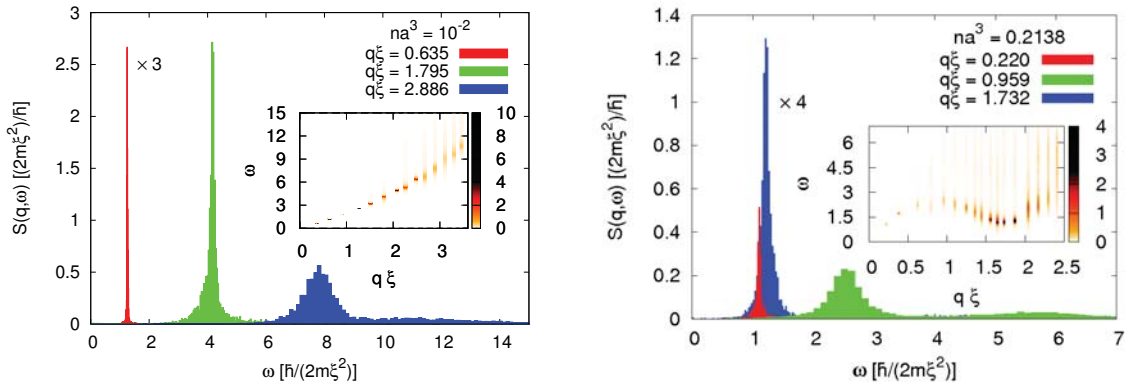

Figure 1. GIFT results for the dynamic structure factor $S(\mathbf{q},\omega)$ at $na^3 = 10^{-2}$ (left panel) and at $na^3 = 0.2138$ (right panel), for three different values of the wave vector q. The peak at $q\xi = 0.635$ in the left panel and the peak at $q\xi = 1.732$ in the right panel have been rescaled by a factor 0.33 and 0.25 respectively. The inset figures show color maps of $S(\mathbf{q},\omega)$ as a function of q.

infinite number of spectral functions which are compatible with a given numerical data set for the imaginary time correlation function.

To tackle this problem, we have used the Genetic Inversion via Falsification of Theories (GIFT) method [15]. The basic idea of this algorithm is that, instead of finding a unique solution for the inverse problem, it explores a wide space of models by means of a genetic algorithm in order to search and collect a large set of spectral functions compatible with a given QMC estimation for $F(\mathbf{q},\tau)$.

The final estimation of $S(\mathbf{q},\omega)$ is obtained averaging all the spectral functions collected: this procedure washes out the unphysical spurious features, which arise from statistical fluctuations, and reinforce the features shared by most of the collected spectral functions, which can be attributed to the real dynamic structure factor.

The GIFT technique has been successfully applied to a number of quantum many-body systems: liquid and solid ^{4}He [15, 27], bosons with soft-core repulsive potentials [28], two-dimensional ^{4}He [29] and two-dimensional normal liquid ^{3}He [30]. In these applications, GIFT has allowed to accurately determine the energy-momentum dispersion relation, $E(\mathbf{q})$, to discern the multi-excitations and to obtain the static density response function, $\chi(\mathbf{q})$ [31, 32, 33]. More details of the GIFT method can be found in Ref. [15].

3. Results

In order to calculate the imaginary time correlation function $F(\mathbf{q},\tau)$ in a HS Bose gas at a given density, we performed PIGS simulations of $N = 400$ particles interacting with the pair potential in Eq. 3 and confined inside a cubic box with periodic boundary conditions. Typical results of the dynamic structure factor obtained with the GIFT algorithm are shown in Fig. 1.

In a regime where the interactions among the particles are moderately weak (gas parameter $na^3 = 10^{-2}$, left panel of Fig. 1), $S(\mathbf{q},\omega)$ presents, at low q, a single narrow peak with a linear dispersion in q: this indicates clearly the excitation of phonons in the quantum system. As the wave vector increases, the excitation peak broadens, suggesting the emergence of physical processes involving the damping of these phonons. For large values of the wave vector ($q\xi \gtrsim 2.886$), $S(\mathbf{q},\omega)$ shows, in addition to the main peak, also a broad tail at high frequencies, indicating the emergence of a multiphonon branch in the spectrum of the excitations.

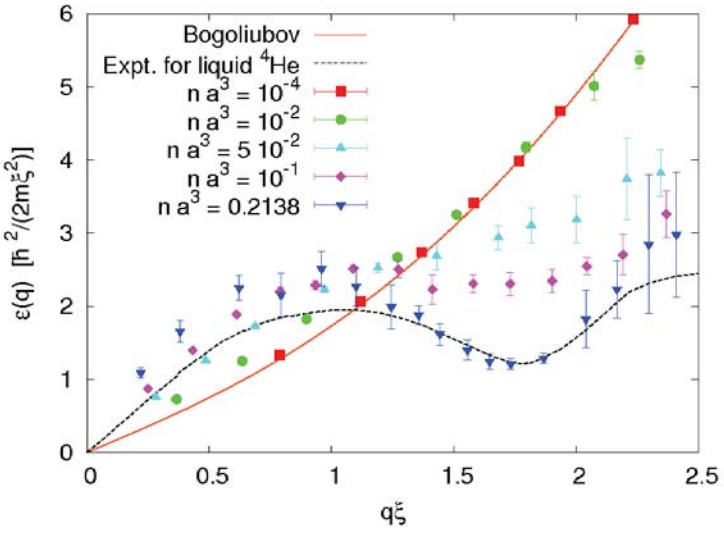

Figure 2. Dispersion of the central position of the main peak in $S(\mathbf{q},\omega)$ for different values of the gas parameter.The orange solid line is the Bogoliubov prediction for the excitation spectrum (Eq. 2) and the black dashed line is the experimental dispersion of the elementary excitations of superfluid ^{4}He at SVP [34]. Where not shown, statistical uncertainties are below the symbol size.

When the interaction strength increases, the behavior of the dynamic structure factor changes notably. In the right panel of Fig. 1, we show $S(\mathbf{q},\omega)$ for the HS gas at the density $na^3 = 0.2138$: this system is particularly interesting since it has been used as a reference system for the simulation of superfluid ^{4}He at saturated vapor pressure (SVP) in a previous work which considers the hard-wall potential as the leading part of the He-He interaction and the attractive tail as a weak perturbation [18]. For small values of the wave vector q, we can see that $S(\mathbf{q},\omega)$ is exhausted by a single sharp peak, whose frequency follows the phonon dispersion $\omega(\mathbf{q}) = cq$ (being c the speed of sound), similarly to the behavior of the dilute gas at low q. However, the broadening of the main peak and the appearance of the multiphonon contribution become relevant already at values of the wave vector which are smaller compared to the case of the dilute gas ($q\xi \gtrsim 0.5$). Furthermore, we notice that the dynamic structure factor shows again a sharp peak for $1.5 \lesssim q\xi \lesssim 2$, indicating the presence of well defined quasiparticles even in this range of wave vectors. The dispersion of these elementary excitations is not monotonous with q, but it displays a relative minimum, showing that the sharp peak in $S(\mathbf{q},\omega)$ can be associated to the excitation of a roton.

The emergence of the roton, as the density of the gas increases, shows up if we plot the dispersion $\varepsilon(\mathbf{q}) = \hbar\omega(\mathbf{q})$ of the main peak of the dynamic structure factor as a function of the wave vector q (Fig. 2). At the lowest gas parameter that we have studied, $na^3 = 10^{-4}$, the dispersion law $\varepsilon(\mathbf{q})$ follows very well the Bogoliubov prediction (Eq. 2). At higher densities, we clearly notice some deviations from this behavior, both for small and large values of q. In the phonon region, we notice that the excitation energy is higher than the one expected from $\varepsilon_B(\mathbf{q})$, indicating that the speed of sound c increases as the density of the gas increases. For wave vectors $1.3 \lesssim q\xi \lesssim 2.5$, instead, we notice that the energy of the excitation decreases for increasing gas parameter. We can also notice that, for $na^3 \simeq 5 \times 10^{-2}$, the spectrum of elementary excitations shows a change of curvature, which develops into a roton minimum when the gas parameter $na^3 \gtrsim 10^{-1}$.

It is interesting to compare the dispersion law of elementary excitations for the HS gas at $na^3 = 0.2138$ (i.e. the gas parameter corresponding to superfluid ^{4}He at equilibrium density) to the one obtained experimentally from inelastic neutron scattering in superfluid ^{4}He [34], which is also shown in Fig. 2. For small wave vectors, our results for the energy of the excitation is larger than the experimental data. This indicates that, as one should expect, the attractive tail of the He-He potential plays a relevant role in determining the speed of sound in the system.

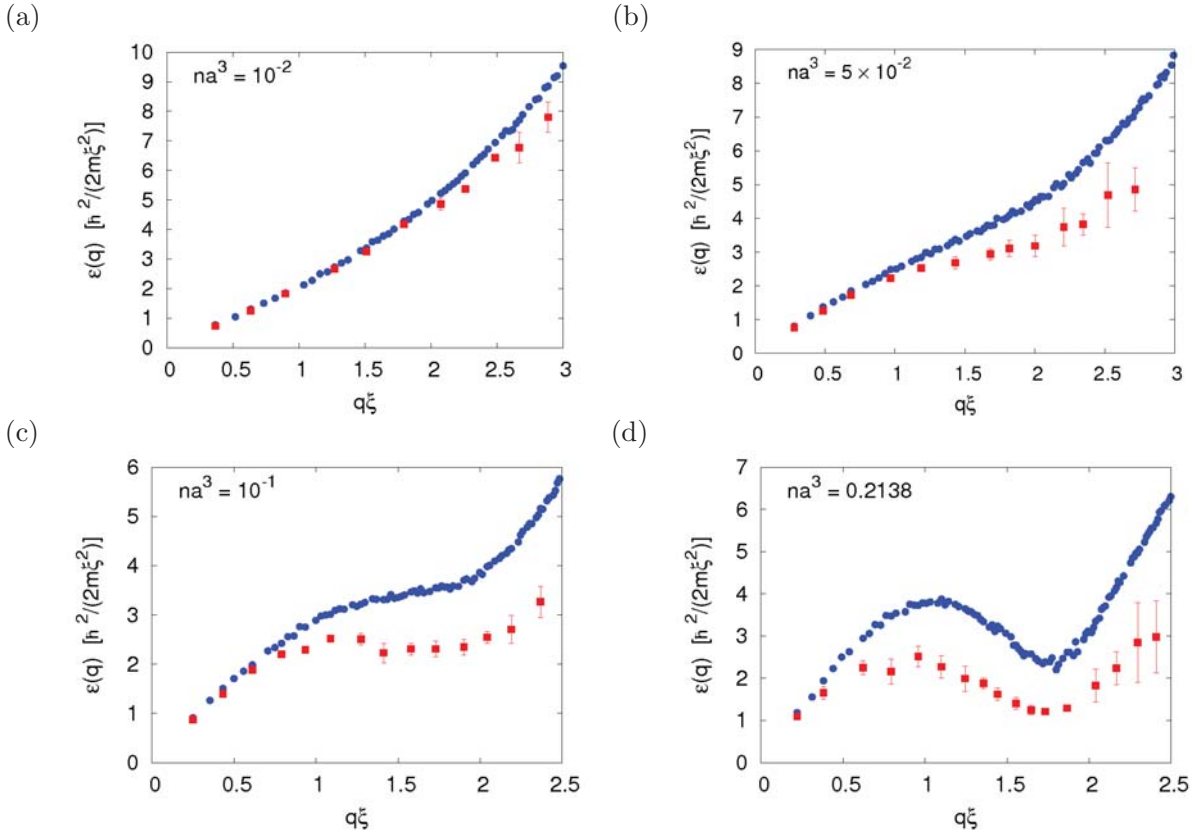

Figure 3. Spectrum of the elementary excitations $\varepsilon(\mathbf{q})$ of the HS-gas for different values of the gas paramenter: $na^3 = 10^{-2}$ (panel a), $na^3 = 5 \times 10^{-2}$ (panel b), $na^3 = 10^{-1}$ (panel c), $na^3 = 0.2138$ (panel d). GIFT results (red squares) are compared with the estimation of $\varepsilon_F(\mathbf{q})$ provided within the Feynman approximation, Eq. 12 (blue circles). Where not shown, statistical uncertainties are below the symbol size.

On the contrary, the dispersion law of elementary excitations obtained with our QMC approach is in good agreement with the experimental measurements in the roton region and for higher momenta: this suggests that the HS model is able to reproduce the density fluctuation spectrum of superfluid ^{4}He for wave vectors reciprocal to the mean interparticle and shorter distances [35].

A qualitative description of the appearance of the roton in the excitation spectrum for increasing na^3 can be obtained via the Feynman's approximation [36]

$$\varepsilon_F(\mathbf{q}) = \hbar\omega_F(\mathbf{q}) = \frac{\hbar^2 q^2}{2mS(\mathbf{q})} \,, \tag{12}$$

in which $S(\mathbf{q})$ is the static structure factor. This relation is easily obtained from the f-sum rule

$$\int_0^\infty d\omega\, \omega S(\mathbf{q},\omega) = \frac{\hbar q^2}{2m} \tag{13}$$

with the assumption that the dynamic structure factor can be written as a single delta-peak $S(\mathbf{q},\omega) = S(\mathbf{q})\delta\left(\omega - \omega_F(\mathbf{q})\right)$ and indicates that the emergence of a minimum in $\varepsilon(\mathbf{q})$ can be associated to the emergence of a maximum in $S(\mathbf{q})$ and thus to the formation of the microscopic local structures typical of dense fluids [35]. In Ref. [37], the excitation spectrum of the HS gas

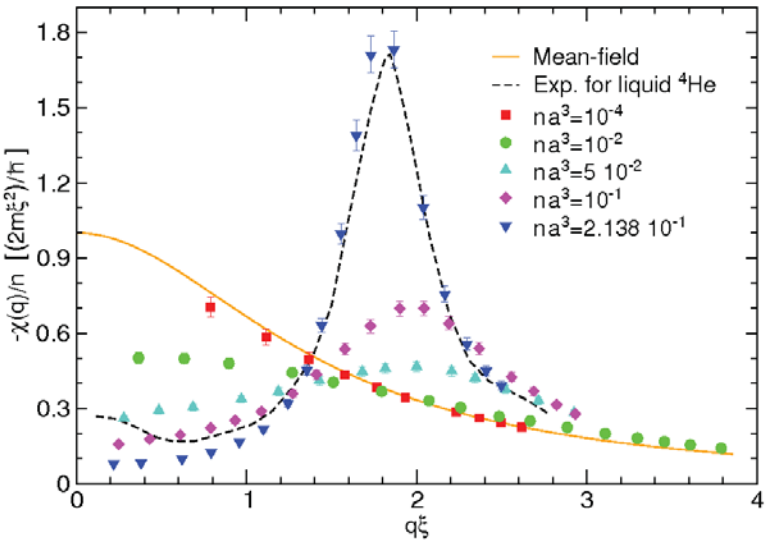

Figure 4. Static density response function $\chi(\mathbf{q})$ for the HS gas at different values of the gas parameter. The orange solid line is the mean-field result for $\chi(\mathbf{q})$ and the black solid line is the experimental static density response function of superfluid ^{4}He at SVP [40]. Where not shown, statistical uncertainties are below the symbol size.

has been obtained from PIGS calculation of $S(\mathbf{q})$, making use of the Feynman's approximation, and it has been shown that, even within this approximated scheme, a roton minimum appears at high density. In order to test this approximation from a quantitative point of view, we compare in Fig. 3 the accurate result for $\varepsilon(\mathbf{q})$, obtained from the GIFT estimation of the dynamic structure factor, with the approximated result $\varepsilon_F(\mathbf{q})$ obtained from the PIGS results for the static structure factor, according to Eq. 12. We can see that the Feynman's approach is able to describe accurately the dynamics of the HS gas only for small values of the wave vector q. At large q, instead, we notice a discprepancy between the Feynman's prediction $\varepsilon_F(\mathbf{q})$ and the GIFT results, which becomes larger as the gas parameter increases. From this comparison, we can conclude that the assumption of describing the dynamic structure factor in terms of a single peak is accurate only in the phonon region, while the secondary multiphonon branch gives a relevant contribution at large wave vectors, especially for strongly interacting systems.

In our study, we also calculate the static density response function $\chi(\mathbf{q})$. This quantity describes the linear response in density to a weak perturbation which is spatially modulated with a wave vector $\mathbf{q}$. In the limit $q \to 0$, $\chi(\mathbf{q})$ converges to the isothermal compressibility [38]. From the knowledge of the dynamic structure factor, the static density response function can be obtained using the following formula:

$$\chi(\mathbf{q}) = -2n \int_0^\infty d\omega \, \frac{S(\mathbf{q},\omega)}{\omega} \, . \tag{14}$$

In figure 4 we present the static density response function calculated from the reconstructed dynamic structure factors of the HS system for different gas parameters. In the weakly interacting regime ($na^3 = 10^{-4}$), $\chi(\mathbf{q})$, for the available wave vectors, is monotonically decreasing, consistently with the behavior of the dilute gas. Comparing our numerical results with the curve for $\chi(\mathbf{q})$ obtained within the mean-field approximation based on the Bogoliubov dispersion (Eq. 2), that is

$$\chi(\mathbf{q}) = \frac{2m\xi^2}{\hbar} \frac{2}{(q\xi)^2 + 2} \, , \tag{15}$$

we notice an excellent agreement at large q, while at small q we find that the QMC estimates are systematically slightly below the mean-field prediction. This discrepancy may be due to finite-size effects, which are not easy to evaluate since the set of the wave vectors q achievable

in our QMC simulations depends on the geometry of the box and thus a calculation of $\chi(\mathbf{q})$ at the same q but with different sizes of the box is not straightforward. However, the statistical uncertainties of our results do not allow to exclude a statistical origin of such discrepancy.

By increasing the gas parameter, we observe a decreasing of the value of $\chi(\mathbf{q})$ at small q, which indicates a decreasing of the compressibility of the gas, while at intermediate values of q, we can see the emergence of a peak, which becomes clear for $na^3 = 10^{-1}$, i.e. the same gas parameter at which the roton minimum appears in $\varepsilon(\mathbf{q})$. The behavior displayed by the static density response function confirms that in a strongly interacting many–body Bose system, characterized by the presence of a hard-core interaction, the preferred modulation of the system, revealed by a peak in $\chi(\mathbf{q})$, corresponds to a wave vector in the vicinity of the roton minimum. Such peak is a precursor of a Bragg–like peak which appears during crystallization [39].

As we did for the dispersion relation of the elementary excitations, it is interesting to compare our numerical result for the static response function of the HS gas at $na^3 = 0.2138$ with the experimental measurements for superfluid ^{4}He at SVP [40]. As we can see in figure 4, there is a significative difference for $q\xi \lesssim 1.4$, which reflects a discrepancy in the compressibility, and thus in the speed of sound (see Fig. 2), between the HS gas and superfluid ^{4}He. On the contrary, we can notice that, for momenta in the roton and post-roton regions, the agreement between the two curves is good. This result confirms the hypothesis that superfluid ^{4}He behaves like a HS system for wave vectors corresponding to the inverse of the mean interatomic distance and above [35].

4. Conclusions

In this work, we have estimated the dynamic structure factor and the spectrum of elementary excitations for Bose HS gases at zero temperature, ranging from the dilute to the dense regime, by means of *ab-initio* calculations based on QMC methodologies. The numerical approach followed, which makes use of the GIFT algorithm to perform the analytical continuation of the "exact" PIGS results for the imaginary time correlation functions, is one of the most powerful methods presently available and allow us to get very accurate results for the spectral functions, even for strongly interacting systems, where it is difficult to describe properly all the relevant correlations arising among the quantum particles. We have been able to see, in the dispersion of the elementary excitations, a crossover from the Bogoliubov spectrum, predicted in mean-field theories and accurate for weakly interacting gases, to the phonon-maxon-roton spectrum, experimentally seen in dense Bose liquids, such as superfluid ^{4}He. We also show that, for large values of the wave vector of the density fluctuation, the dynamic structure factor presents a broad multiphonon contribution at high frequencies, which becomes relevant as the density of the system increases, making quantitatively inaccurate the Feynman's approximation for the spectrum of the elementary excitations. Remarkably, for $na^3 = 0.2138$, the gas parameter corresponding to superfluid ^{4}He at equilibirum density, the hard-sphere model turns out to describe accurately the energy–momentum dispersion relation and the static density response of superfluid ^{4}He in the roton region; this suggests that, for wavelengths comparable to interatomic distances, the low–energy dynamic properties are dominated by the hard-core repulsive part of the interaction potential.

Acknowledgments

This work has been supported by Regione Lombardia and CINECA Consortium through a LISA Initiative (Laboratory for Interdisciplinary Advanced Simulation) 2012 grant [http://www.hpc.cineca.it/services/lisa], by ERC through the QGBE grant and by Provincia Autonoma di Trento. Partial support by the Italian MIUR under Contract Cofin-2009 "Quantum gases beyond equilibrium" is also acknowledged. We thank the Aurora-Science project (funded

by PAT and INFN) for allocating part of the computing resources for this work and for technical support.

References

[1] Glyde H R 1994 *Excitations in Liquid and Solid Helium* (Oxford: Clarendon Press)
[2] Dalfovo F, Giogrini S, Pitaevskii L P and Stringari S 1999 *Rev. Mod. Phys.* **71** 463
[3] Steinhauer J, Ozeri R, Katz N and Davidson N 2002 *Phys. Rev. Lett.* **88** 120407
[4] Svensson E C, Martel P, Sears V F and Woods A D B 1976 *Can J. Phys* **54** 2178
[5] Talbot E F, Glyde H R, Stirling W G and Svensson E C 1988 *Phys. Rev. B* **38** 11229
[6] Stirling W G and Glyde H R 1990 *Phys. Rev. B* **41** 4224
[7] Andersen K H, Stirling W G, Scherm R, Stunault A, Fak B, Godfrin H and Dianoux A J 1994 *J. Phys: Condensed Matter* **6** 821
[8] Andersen K H and Stirling W G 1994 *J. Phys: Condensed Matter* **6** 5805
[9] Gibbs M R, Andersen K H, Stirling W G and Schober H 1999 *J. Phys: Condensed Matter* **11** 603
[10] Sarsa A, Schmidt K E and Magro W R 2000 *J. Chep. Phys* **113** 1366
[11] Ceperley D M 1995 *Rev. Mod. Phys.* **67** 279
[12] Jarrell M and Gubernatis J E 1996 *Phys. Rep.* **269** 133
[13] Boninsegni M and Ceperley D M 1996 *J. Low Temp. Phys* **104** 339
[14] Baroni S and Moroni S 1999 *Phys. Rev. Lett.* **82** 4745
[15] Vitali E, Rossi M, Reatto L and Galli D E 2010 *Phys. Rev. B* **82** 174510
[16] Huang K and Yang C N 1957 *Phys. Rev.* **105** 767
[17] Hansen J P, Levesque D and Shiff D 1971 *Phys. Rev. A* **3** 776
[18] Kalos M H, Levesque D and Verlet L 1957 *Phys. Rev. A* **9** 2178
[19] Giorgini S, Boronat J and Casulleras J 1999 *Phys. Rev. A* **60** 5129
[20] Rossi M, Nava M, Reatto L and Galli D E 2009 *J. Chem. Phys.* **131** 154108
[21] Zillich R E, Mayrhofer J M and Chin S A 2010 *J. Chem. Phys.* **132** 044103
[22] Cao J and Berne B J 1992 *J. Chem. Phys.* **97** 2382
[23] Boninsegni M, Prokof'ev N V and Svistunov B V 2006 *Phys. Rev. Lett.* **96** 070601
[24] Rota R, Casulleras J, Mazzamti F and Boronat J 2010 *Phys. Rev. E* **81** 016707
[25] Pollock E L and Ceperley D M 1984 *Phys. Rev. B* **30** 2555
[26] Pollock E L and Ceperley D M 1987 *Phys. Rev. B* **36** 8343
[27] Rossi M, Vitali E, Reatto L and Galli D E 2012 *Phys. Rev. B* **85** 014525
[28] Saccani S, Moroni S and Boninsegni M 2012 *Phys. Rev. Lett.* **108** 175301
[29] Arrigoni F, Vitali E, Galli D E and Reatto L 2013 *Low Temp. Phys.* **39** 793 [*Fiz. Niz. Temp.* **39**, 1021]
[30] Nava M, Galli D E, Moroni S and Vitali E 2013 *Phys. Rev. B* **87** 144506
[31] Minoguchi T and Galli D E 2011, *J. low temp phys* **162**, 160
[32] Minoguchi T, Galli D E, Rossi M, and Yoshimori A 2012, *J. Phys.: Conf. Ser.* **400**, 012050
[33] Minoguchi T, Nava M, Tramonto F and Galli D E 2013, *J. Low. Temp. Phys.* **171**, 259
[34] Donnelly R J, Donnelly J A and Hills R N 1981 *J. Low Temp. Phys.* **44** 471
[35] Rota R, Tramonto F, Galli D E and Giorgini S 2013 *Phys. Rev. B* **88**, 214505
[36] Feynman R P 1954 *Phys. Rev.* **94** 262
[37] Rossi M and Salasnich L 2013 *Phys. Rev. A* **88** 053617
[38] See *e.g.* Pitaevskii L and Stringari S 2003 *Bose-Einstein Condensation* (Oxford: Clarendon Press).
[39] Vitali E, Galli D E, and Reatto L 2008, in *Advanced in Quantum Many-body Theory* **11**, 251
[40] Cowley R A and Woods A D B 1971, *Cam. J. Phys.* **49**, 187